Wireless Theranostic Smart Contact Lens for Monitoring and Control of Intraocular Pressure in Glaucoma

Tae Yeon Kim[1], Jee Won Mok[3], Sang Hoon Hong[1], Sang Hoon Jeong[1], Hyeon Sik Choi[2], Sangbaie Shin[2], Choun-Ki Joo[3] and Sei Kwang Hahn[1,2]*

[1] Department of Materials Science and Engineering, Pohang University of Science and Technology (POSTECH), 77 Cheongam-ro, Nam-gu, Pohang, Gyeongbuk 37673, Korea.

[2] PHI BIOMED Co., #613, 12 Gangnam-daero 65-gil, Seocho-gu, Seoul 06612, Korea.

[3] CK St. Mary's Eye Center, CK building, 559, Gangnam-daero, Seocho-gu, Seoul 06531, Korea.

*** CORRESPONDING AUTHOR FOOTNOTE**

Tel.: +82 54 279 2159; Fax: +82 54 279 2399; E-mail address: skhanb@postech.ac.kr (S. K. Hahn)

Supplementary Methods

Synthesis of AgNW and Ag@AuNW

Silver nanowire was synthesized as a template by the slightly modified polyol method. In brief, EG (65 ml) was heated at 175 °C for 1 h with 0.034 M of PVP (Mw, 360000, Sigma-Aldrich). After heating, 400 μl of 4 mM $CuCl_2$ (Sigma-Aldrich) was added and heated for 10 min. Then, 15 ml of 0.095 M $AgNO_3$ (Sigma-Aldrich) was injected with a syringe pump for 10 min. The reaction was conducted for 20 min and the resulting AgNW was washed multiple times with centrifugation. Ag@AuNW was synthesized by non-galvanic growth of Au on the silver nanowire. The growth solution was prepared by mixing 1.4 ml of 0.2 M hydrogen tetrachloroaurate (III) hydrate ($HAuCl_4 \cdot xH_2O$) (Alfa Aesar), 105 ml of 0.01 M Na_2SO_3 (Sigma-Aldrich) in 165 ml of deionized (DI) water and left for 12 h. After 12 h, the separation solution was prepared by mixing 70 ml of 50 wt% PVP (Mw; 40000, Sigma-Aldrich), 14 ml of 0.5 M NaOH (Sigma-Aldrich), 14 ml of 0.5 M L-ascorbic acid (L-AA, Sigma-Aldrich) and 3.5 ml of 0.1 M Na_2SO_3 in 320 ml DI water. The growth solution was added into the separation solution and the pH of the mixed solution was adjusted by adding 0.2 M NaOH. When the pH was saturated at 10, the silver nanowire solution with a different concentration was added into the mixed solution. The reaction was carried out for 2 h and the synthesized Ag@AuNW was washed with ethanol multiple times.

Preparation of glaucoma induced rabbits

In vivo tests were performed with 15 male New Zealand White rabbits weighing 1.7 to 2.5 kg with no signs of ocular inflammation. All animal experimentation adhered to the ARVO Statement for the use of Animals in Ophthalmic and Vision Research with the approval by the Institutional Care and Use Committee (CRONEX-IACUC: 202110005, CRONEX, Korea). Glaucoma was induced

in both eyes of each animal under sterile condition. Rabbits were anaesthetized with ketamine (50 mg/kg) and Rompun (10 mg/kg) administered intramuscularly. Then, 0.5% alkyne eye drops were applied by topical instillation. After anesthetization of the animals, 2% methyl cellulose (M0512, viscosity of 4,000cP, Sigma-Aldrich) was injected into the anterior chamber with a 29-gauge needle of an insulin syringe and 50 U α-chymotrypsin (from bovine pancreas, C4129, Sigma-Aldrich) into the posterior chamber [1]. Both eyes before each IOP measurement were anesthetized by one drop of 0.5 % alkyne. The first measurement was taken before IOP induction and the second was taken after 1 h. After that, IOP measurements were repeated with a tonometer twice a day, and an average of five IOP readings was used for the analysis. IOP measurements were performed before and after treatment with topical eye drops or drug delivery by wearing the smart contact lens. Glaucoma therapeutic eye drop (0.5% Timoptic, Bausch Lomb) into the right eye and saline instilled into the left eye were performed twice a day.

Corneal Fluorescein Staining

The cornea was stained with fluorescein paper strips (0.4M disodium fluorescein, HAAG-STREI DIAGNOSITECS) soaked in a drop of 0.5 % alkyne. After staining, it was washed with saline solution. The eyes of all animals were examined under a slit-lamp microscope (Keeler, UK) with a cobalt blue filter [2].

Histopathologic and Immunohistochemical Analyses

Formalin-fixed whole eyes were embedded in paraffin for the preparation of 5 μm sections. For histological evaluation, the sectioned tissues were stained with hematoxylin and eosin (H & E; ABCAM, UK) and examined under a direct light microscope. Briefly, immunohistochemical

63 detection included antigen retrieval in 10 mM citrate buffer in a microwave oven and blocking
64 endogenous peroxidase with 1% hydrogen peroxide. Tissues were incubated at 4 °C overnight
65 with the following primary antibodies; GFAP (sc-51908, Santa Cruz), CD11b (ab8878, ABCAM),
66 BDNF (ab108619, ABCAM) and Brn3a (ab345230, ABCAM). Then, the VECTASTAIN Elite
67 ABC reagent (horse anti-mouse/rabbit IgG, Vector Laboratories, Burlingame, CA) for horseradish
68 peroxidase was used for immunohistochemistry. After that, tissues were incubated in a peroxidase
69 substrate solution (ImmPACT® DAB Substrate, Peroxidase, Vector Laboratories, Burlingame, CA)
70 until desired stain intensity developed and were lightly counterstained with nuclear fast red
71 (Abcam, UK).
72
73 **Calibration of IOP level (mmHg) measured by smart contact lens**
74 To obtain the standard graph of each rabbit to convert code change to IOP level, the base codes of
75 smart contact lens were measured before wearing smart contact lens without any tension (0 mmHg,
76 C_0). The IOP level of each rabbit was measured by tonometer (χ mmHg). Right after that, the code
77 outputs were measured by wearing smart contact lens (χ mmHg, C). The code changes obtained
78 by equation (1) were matched with IOP changes with more than 2 points. The slope of standard
79 graph of each rabbit was used to convert code changes (%) to IOP changes (mmHg) for each rabbit
80 using equation (2).

81 $$\Delta C = Code\ change\ (\%) = \frac{(C - C_0)}{C_0} * 100 \qquad (1)$$

82 $$\Delta P = IOP\ change\ (mmHg) = \frac{\Delta C}{S} \qquad (2)$$

83 $$S = Slope\ of\ standard\ graph\ of\ each\ rabbit$$

Before wearing contact lens, the initial IOP was measured by tonometer (P_0). The IOP changes converted by equation (2) were measured with smart contact lens and the IOP level which was desired to measure was calculated by equation (3). Finally, the IOP level measured by smart contact lens was compared to IOP level measured by tonometer right after remove the contact lens.

$$P = P_0 + \frac{\Delta C}{S} = P_0 + \Delta P \qquad (3)$$

Thermal analyses of theranostic smart contact lens

The thermal characterization of theranostic smart contact lens was carried out with the infrared camera for the temperature changes of IOP sensor, antenna, chip and DDS during *in vivo* tests. Although the temperature of chip increased up to 39.3 $^{\circ}$C, there were not any critical thermal damages on the cornea after finishing all *in vivo* tests.

Statistical analysis

We performed one-sided statistical analyses using one-way analysis of variance (ANOVA). For all experiments, *P < 0.05, **P < 0.01 and ***P < 0.001 were considered statistically significant.

Supplementary References

1. Zhu, M. D. & Cai, F. Y. Development of experimental chronic intraocular hypertension in the rabbit. *J Ophthalmol*. **20,** 225-34 (1992).
2. Bron, A. J. et al. Grading of corneal and conjunctival staining in the context of other dry eye tests. *Cornea* **22**, 640–650 (2003).

Supplementary Figures

Supplementary Figure 1. Photo-images of the nanowire solutions of AgNW, Ag@AuNW and AuHNW.

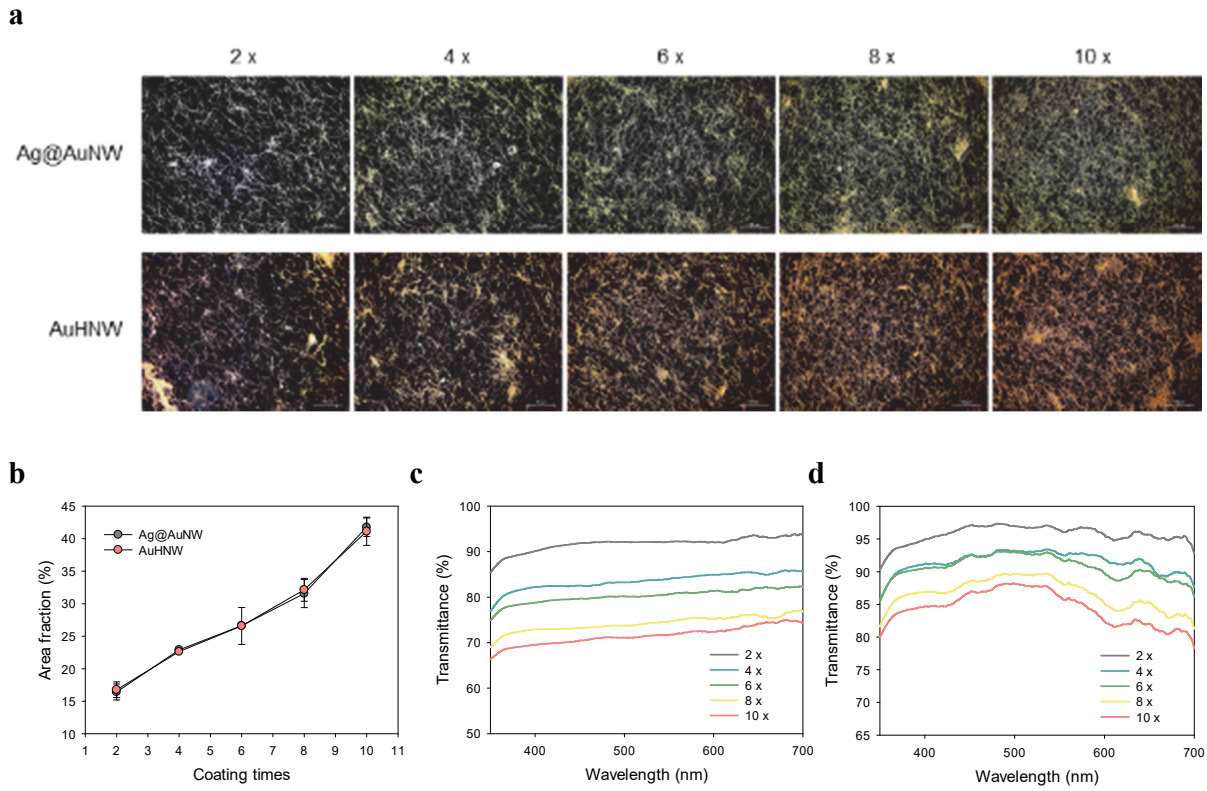

112

113 **Supplementary Figure 2. The area fraction and transmittance of Ag@AuNW and AuHNW.**

114 **a,** OM dark field images of nanowire films with increasing coating times. **b,** The area fraction of

115 nanowire films with increasing coating times. The transmittance spectrum of **c,** Ag@AuNW and

116 **d,** AuHNW films with increasing coating times.

117

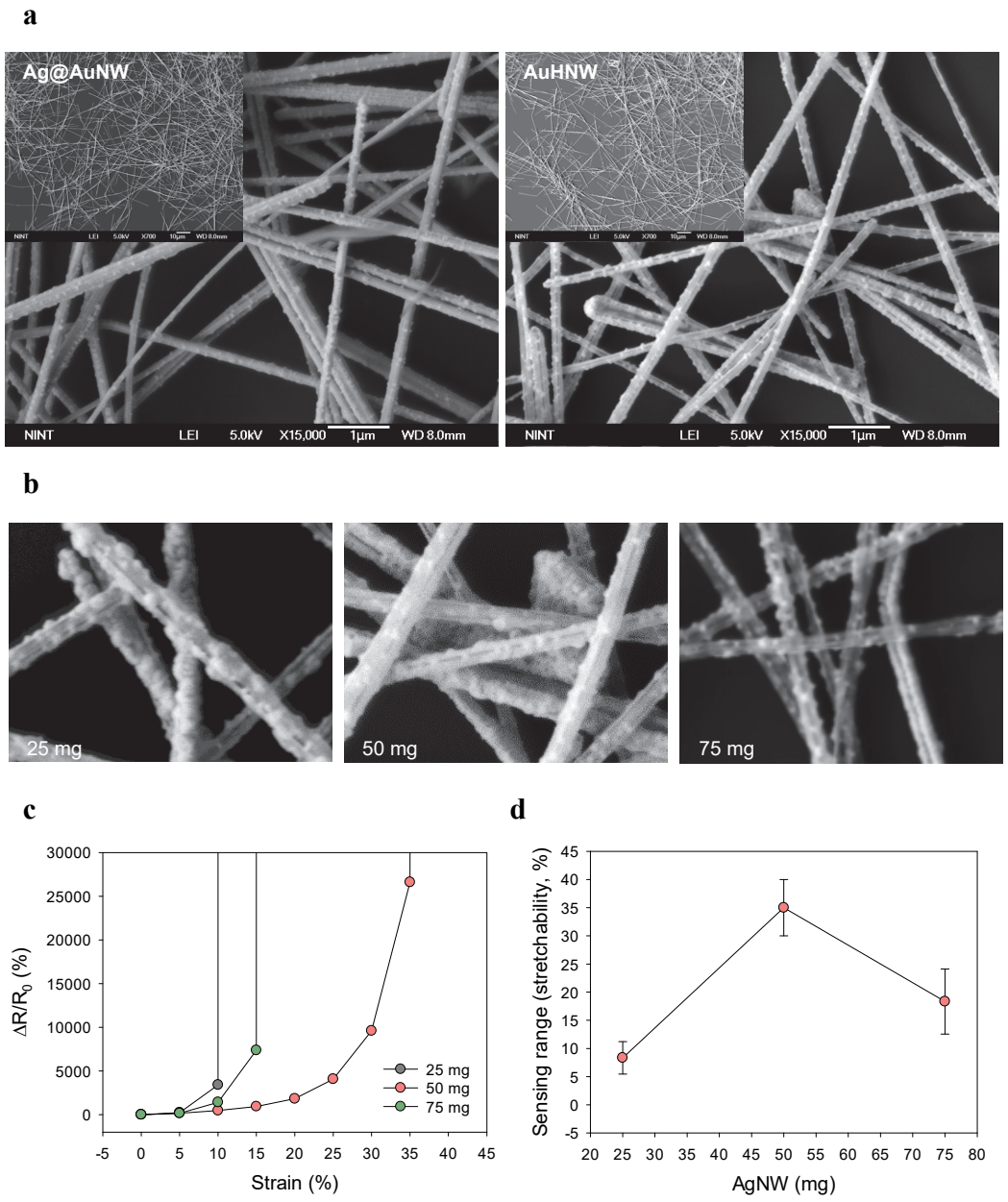

118

119 **Supplementary Figure 3. SEM images and electromechanical properties of AuHNWs.**
120 **a,** SEM images of Ag@AuNW and AuHNW. **b,** SEM images of AuHNW with different template
121 concentrations for tunning the shell thickness. **c,** The relative resistance changes of AuHNW with
122 different template concentrations. **d,** The sensing range of AuHNW with increasing concentration
123 of AgNW templates.

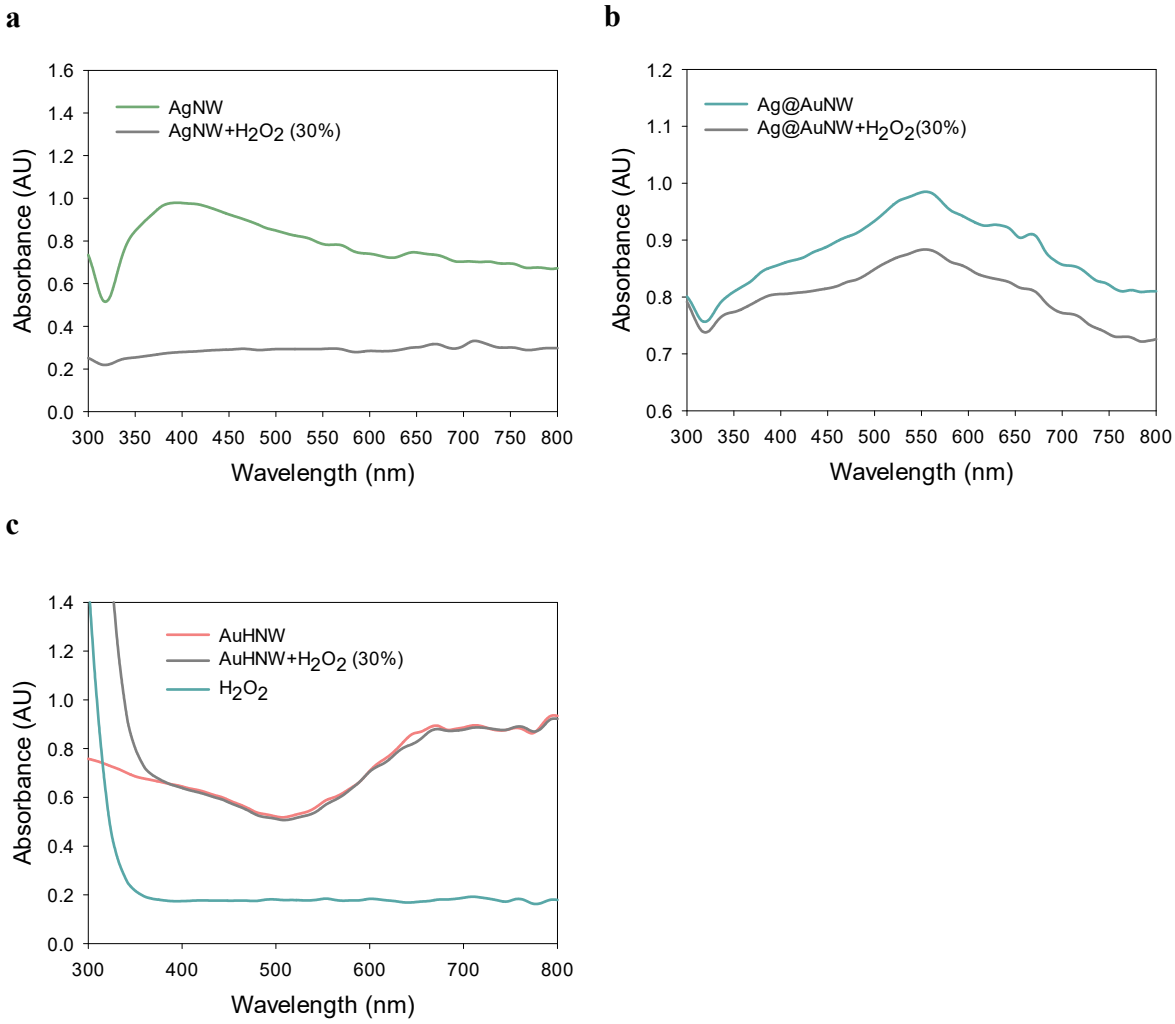

124

125 **Supplementary Figure 4. Hydrogen peroxide exposure tests to assess the chemical stability.**

126 The absorbance change of **a,** AgNW, **b,** Ag@AuNW and **c,** AuHNW after exposure to H_2O_2 (30 %)

127 for 2 h.

128

129

130

131

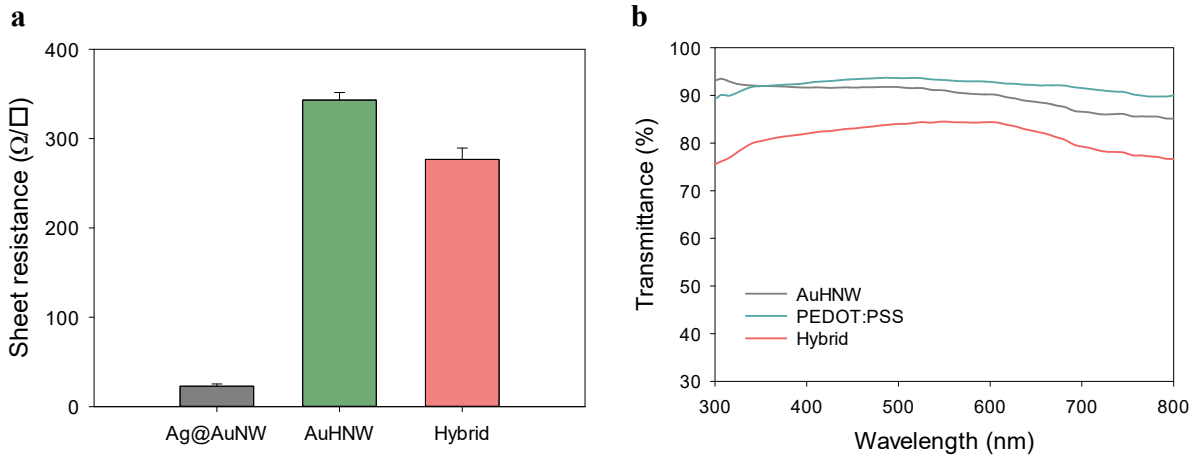

132

133 **Supplementary Figure 5. Electrical and optical properties of hybrid IOP sensor. a,** The sheet

134 resistance and **b,** transmittance of the specified nanomaterials.

135

136

137

138

139

140

141

142

143

144

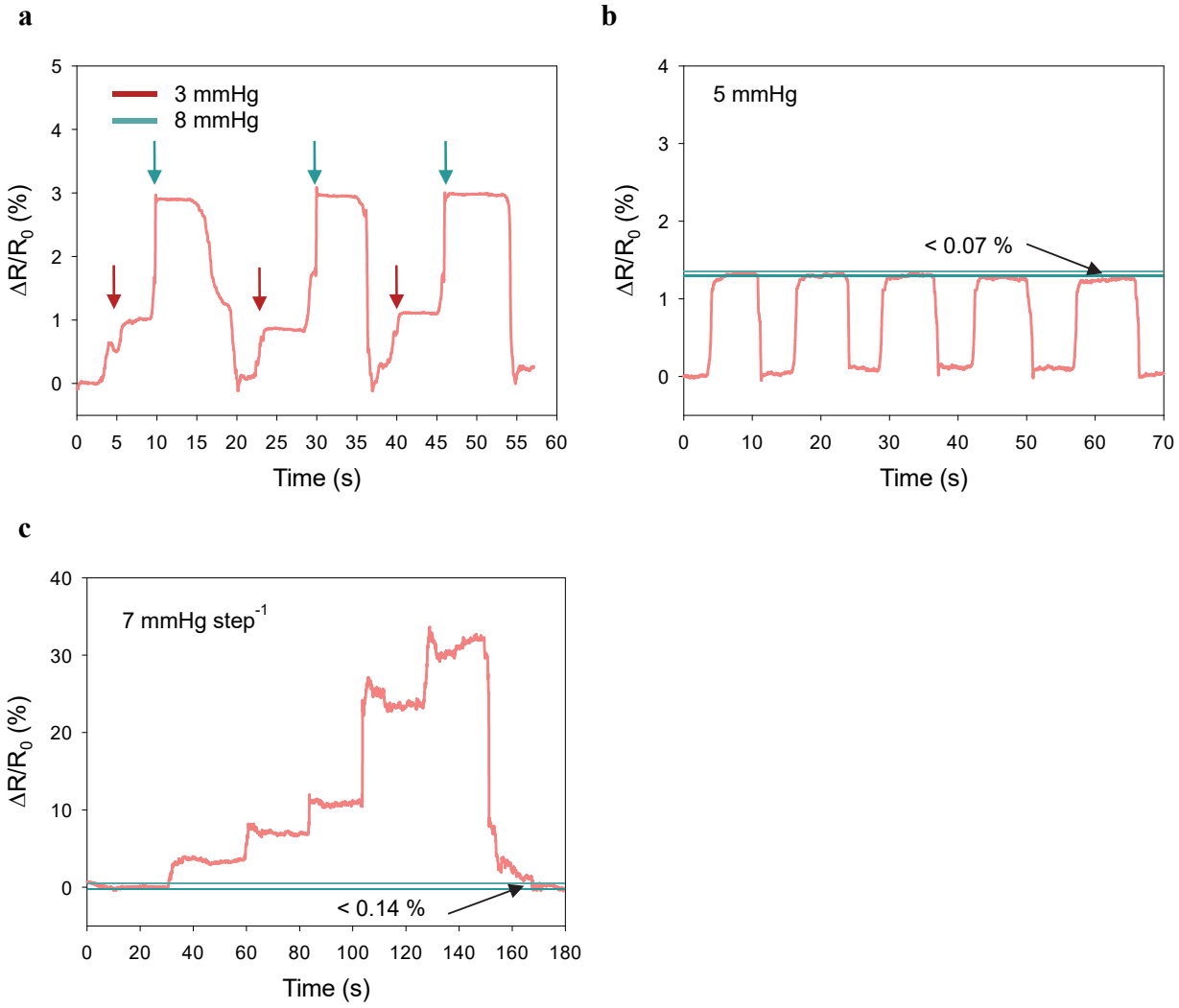

Supplementary Figure 6. Characteristics of the IOP sensor embedded into smart contact lens. **a,** The real time relative resistance change under the different applied IOP change. **b,** The repeated IOP change. **c,** The hysteresis of IOP sensor by applying IOP up to 35 mmHg and recovering to 0 mmHg.

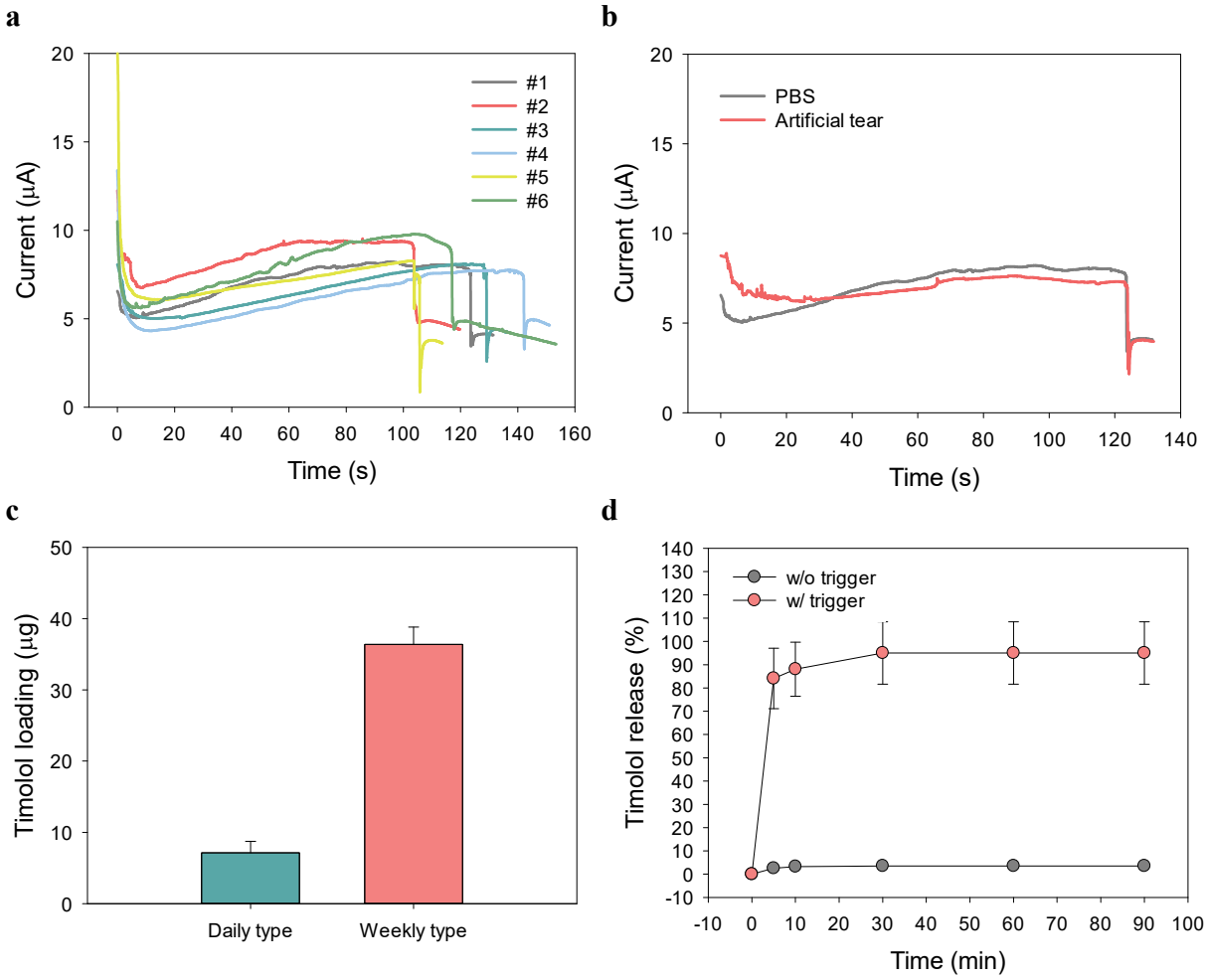

153

154 **Supplementary Figure 7. Characteristics of flexible DDS. a,** The current-time (I-t) curve of
155 each reservoir of flexible DDS in pH 7.4 PBS with applying a constant voltage of 1.85 V. **b,** The
156 electrochemical dissolution of DDS in PBS and artificial tear. **c,** The timolol loading amount for
157 the different type of DDS. **d,** The timolol release profiles released from the flexible DDS.

158

159

160

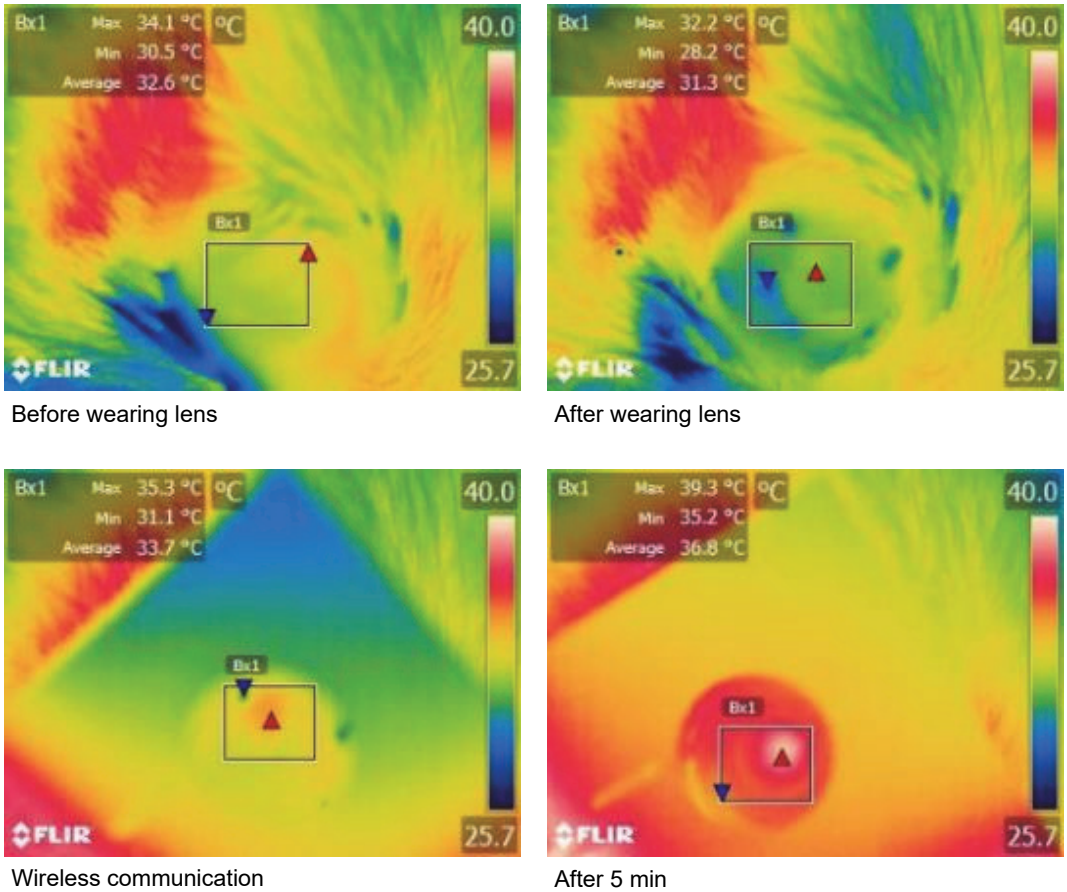

Supplementary Figure 8. The thermal characterization of theranostic smart contact lens.

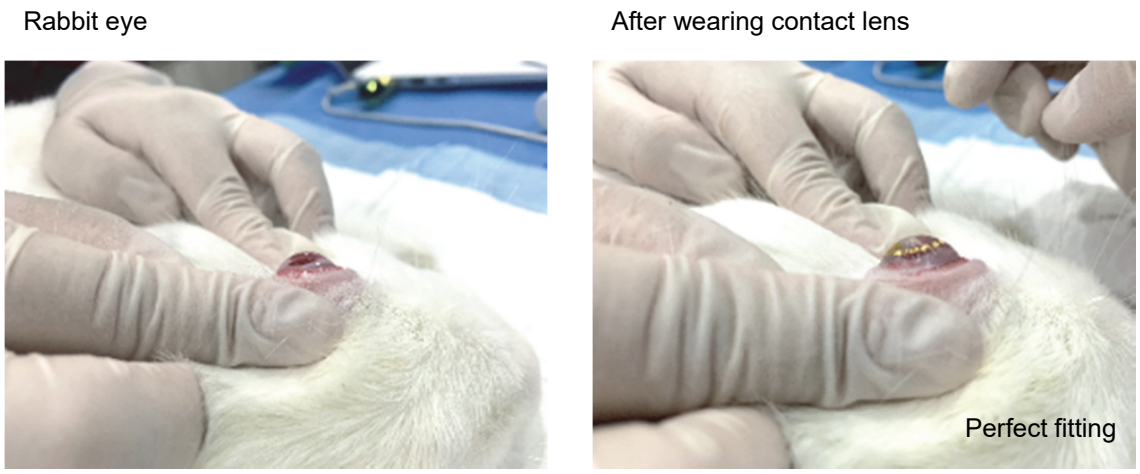

Supplementary Figure 9. The perfect fitting of theranostic smart contact lens on the rabbit eye.

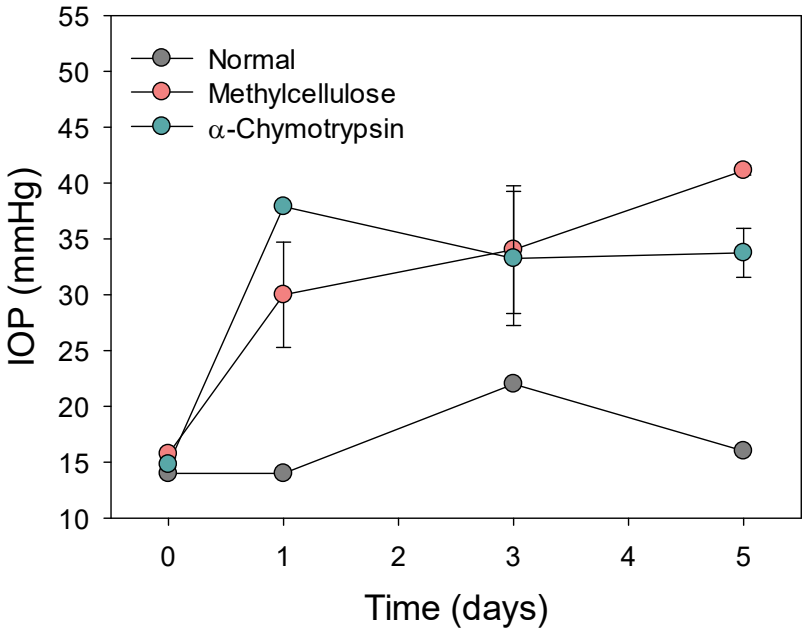

183

184 **Supplementary Figure 10.** The IOP value change of glaucoma induced rabbits by a tonometer.

185

186

187

188

189

190

191

192

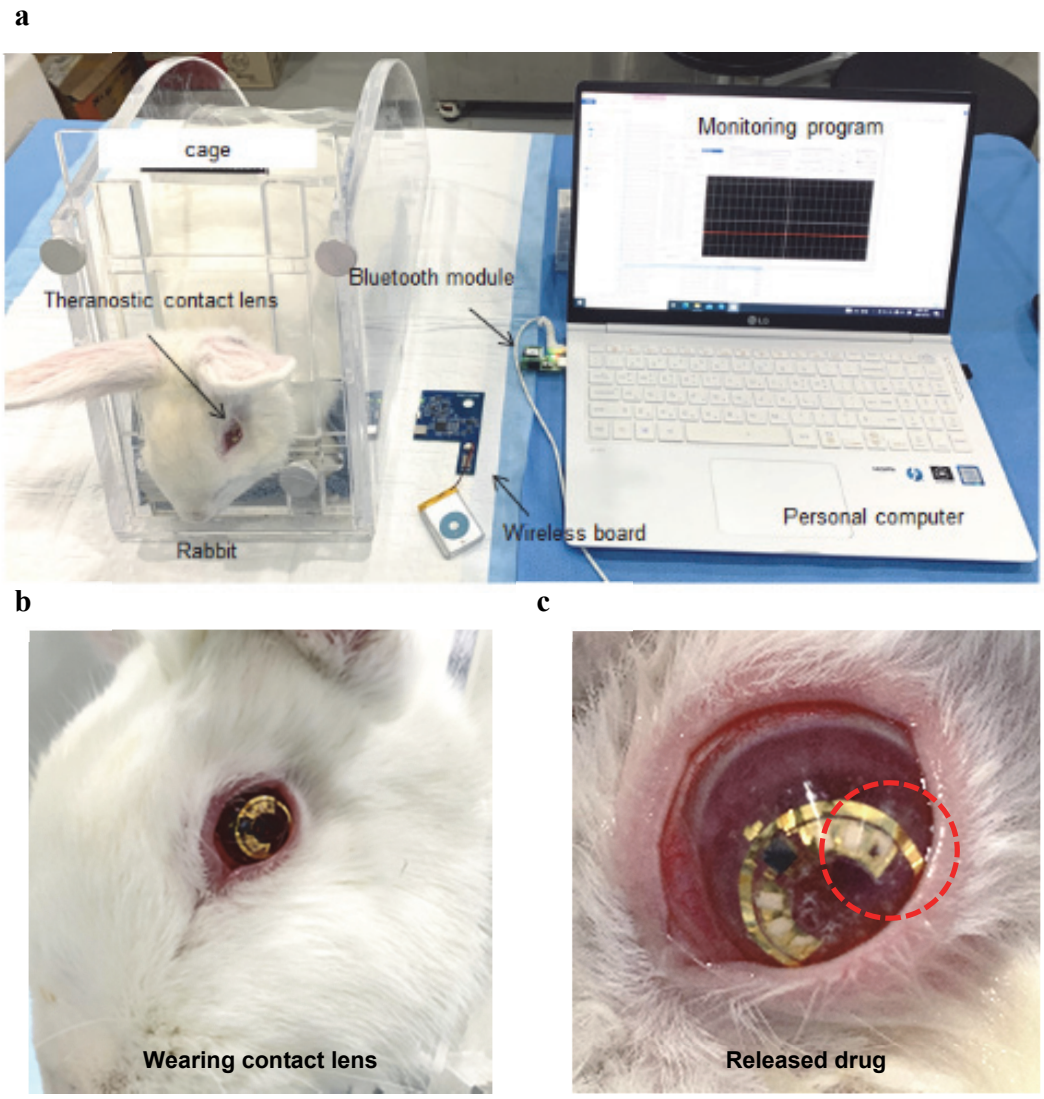

Supplementary Figure 11. ***In vivo*** **test set up with wireless theranostic smart contact lens.** **a,** *In vivo* test set up of theranostic smart contact lens for IOP sensing and drug delivery. Photo-image of rabbits **b,** wearing the smart contact lens, and **c,** smart contact lens on a rabbit eye after drug release.

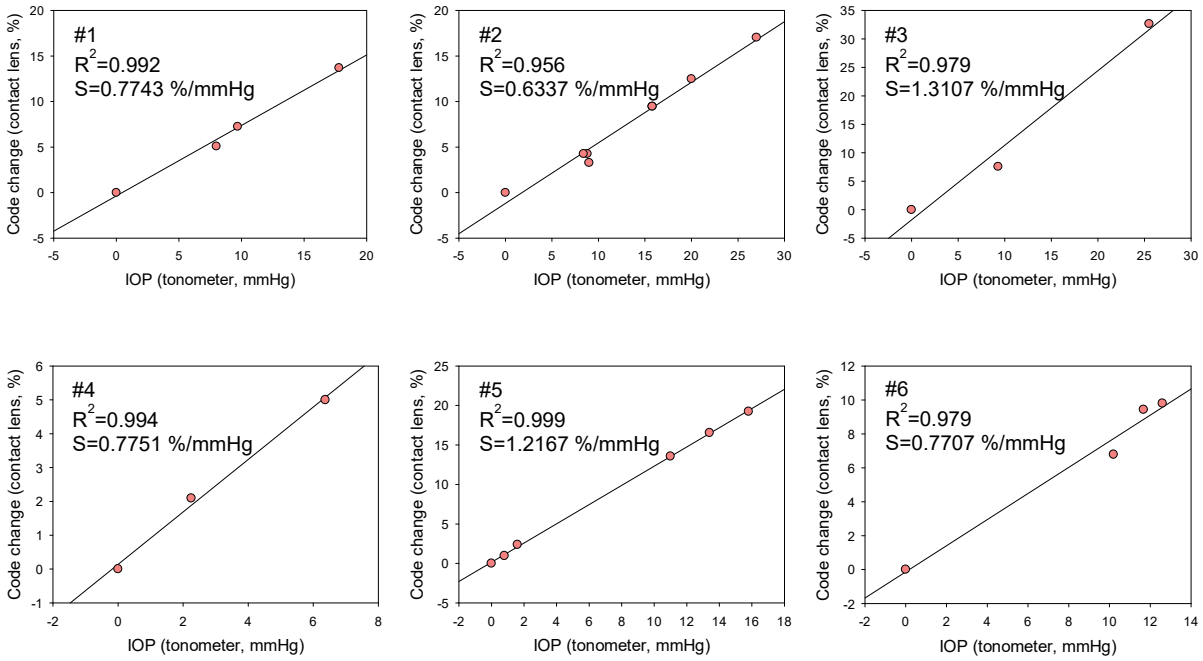

Supplementary Figure 12. The correlation curve between code changes and IOP values of glaucoma induced rabbits. These standard graphs were used for the calibration of smart contact lens for the code change into the IOP value.

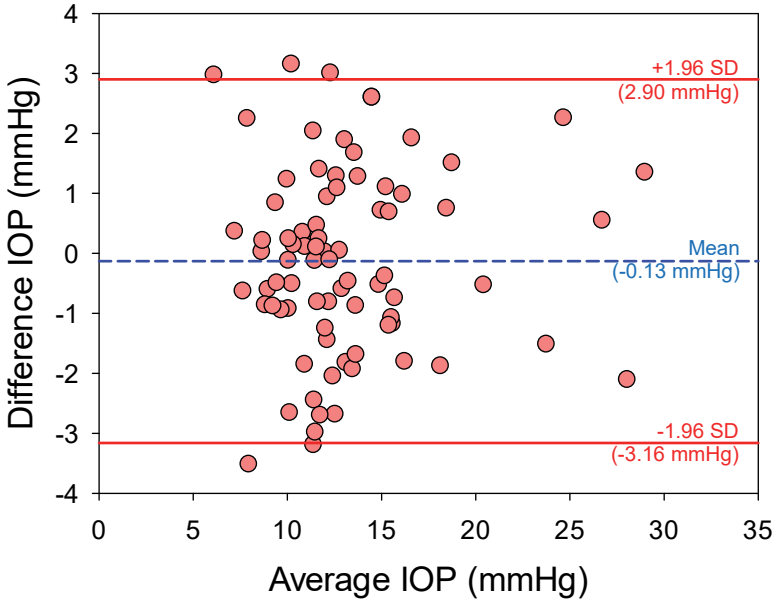

Supplementary Figure 13. Bland-Altman plot between a smart contact lens and a tonometer.

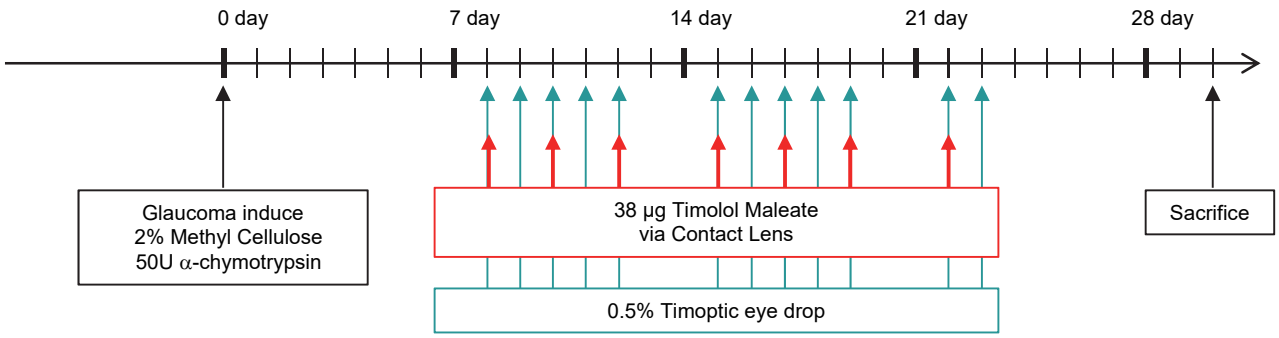

Supplementary Figure 14. *In vivo* test protocol for the assessment of therapeutic effects of theranostic smart contact lens.

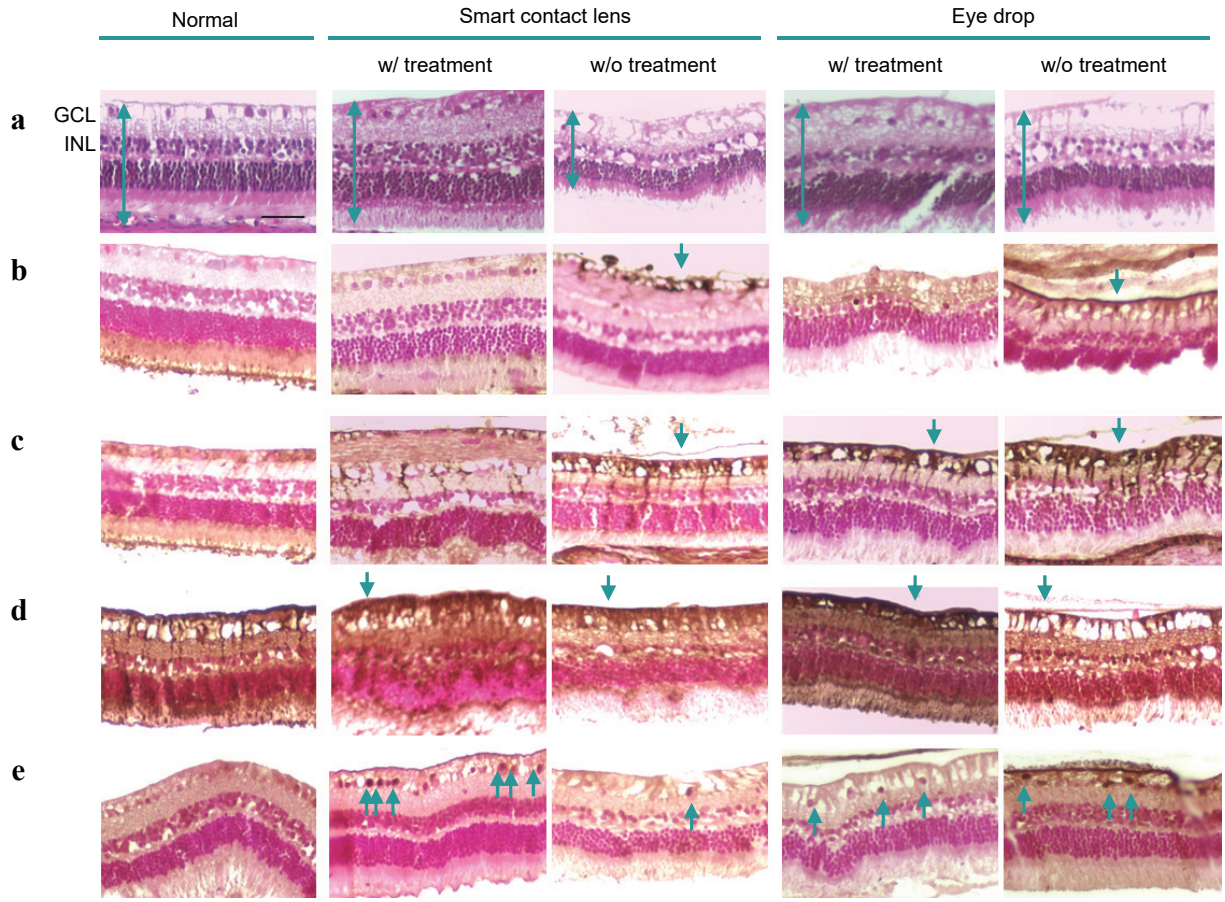

Supplementary Figure 15. ***In vivo*** **therapeutic effect by theranostic smart contact lens and eye drop in glaucoma rabbits induced by methylcellulose. a**, OM images for retinal histology. OM images for immunohistochemical analyses for **b**, GFAP, **c**, CD11b, **d**, BDNF and **e**, Brn3a. Arrows indicate the expression of each marker (scale bar, 100 μm).

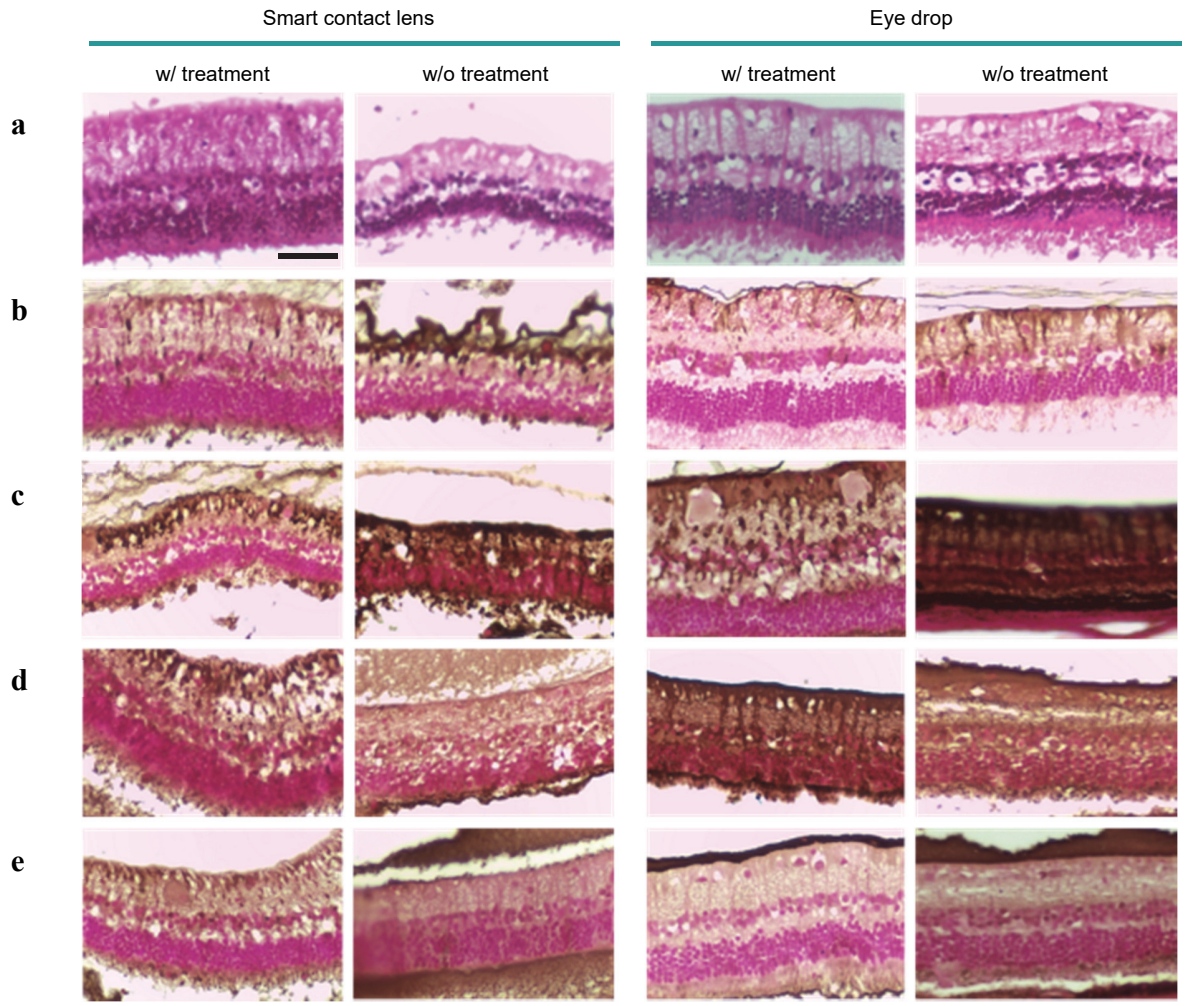

Supplementary Figure 16. ***In vivo*** **therapeutic effect of theranostic smart contact lens and eye drops in glaucoma rabbits induced by α-chymotrypsin. a,** OM images of retinal histology. OM images for immunohistochemical analyses with **b,** GFAP, **c,** CD11b, **d,** BDNF and **e,** Brn3a (scale bar, 100 μm).

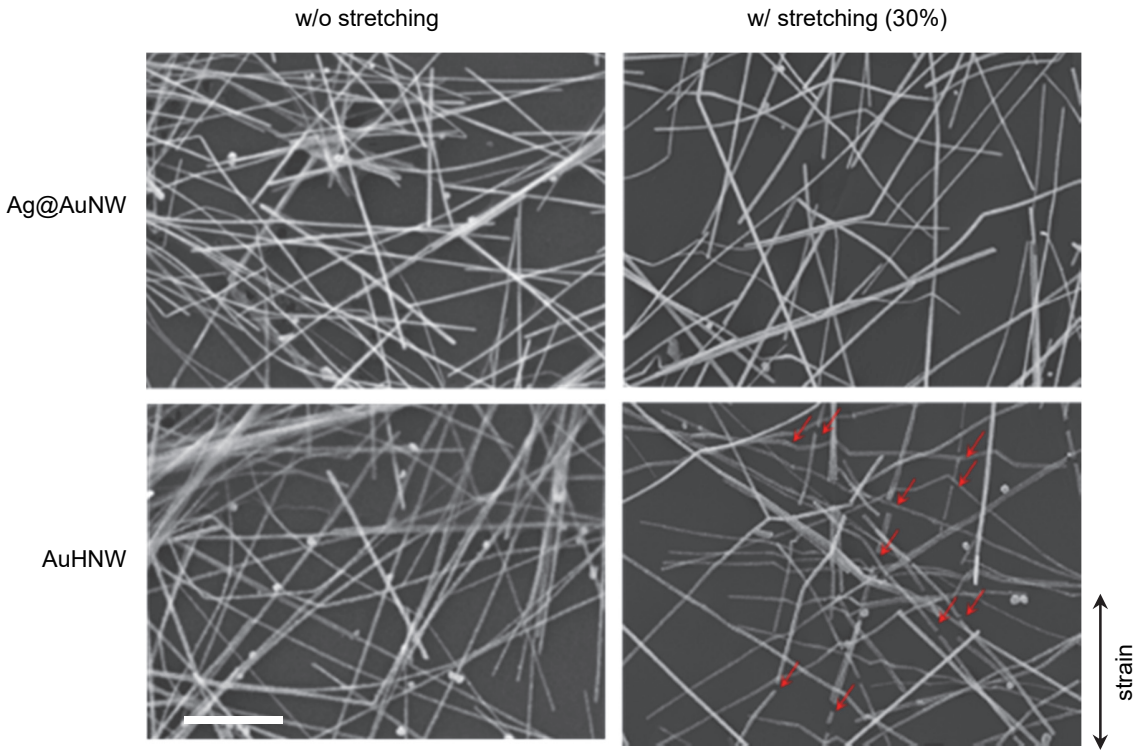

255

256 **Supplementary Figure 17. SEM images of Ag@AuNW and AuHNW with and without**
257 **applying strain.** While there was no critical change in Ag@AuNW with mechanical stretching,
258 cracks were observed through the strain direction in AuHNW with the applied strain. This fracture
259 of AuHNW with strain resulted in the high sensitivity and reasonable stretchability of IOP sensor.
260 Red arrows indicate the cracks of AuHNW (scale bar, 5 μm).

261

262

263

264

265

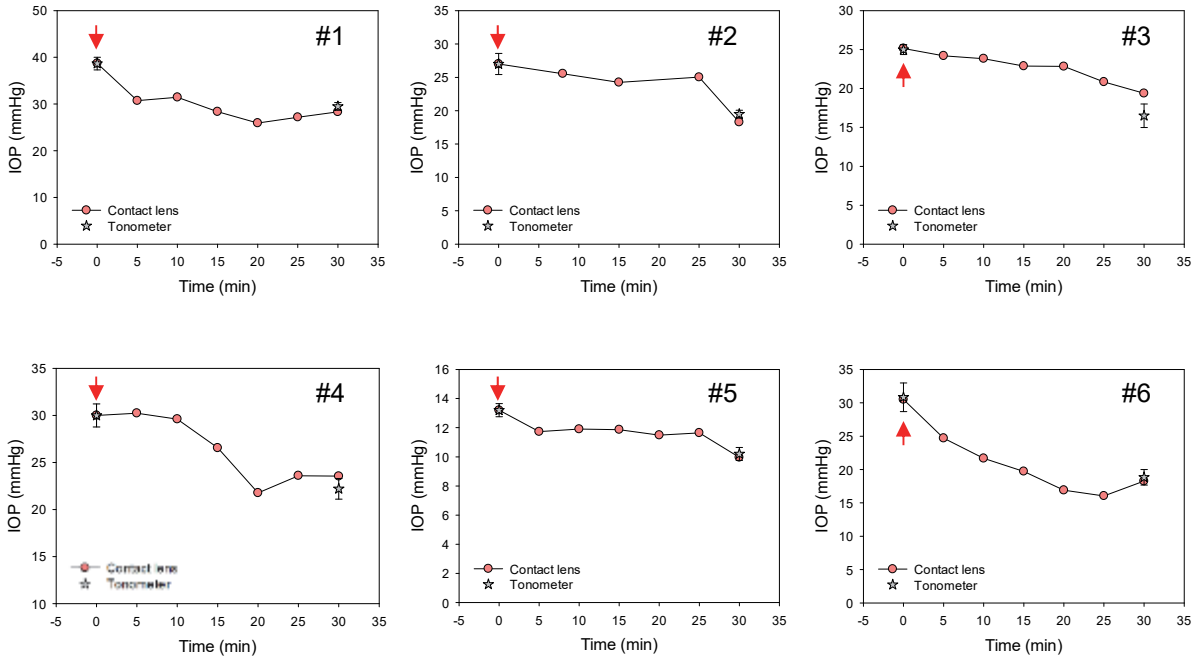

Supplementary Figure 18. The IOP change of glaucoma induced rabbits with drug treatment of theranostic smart contact lens. The IOP was successfully reduced by the treatment of drugs released from theranostic smart contact lens. The trend of IOP reduction was slightly different for each rabbit due to the different drug response or physiological condition.